

MIT Open Access Articles

*Pulsed laser noise analysis and pump-probe
signal detection with a data acquisition card*

The MIT Faculty has made this article openly available. **Please share**
how this access benefits you. Your story matters.

Citation: Werley, Christopher A., Stephanie M. Teo, and Keith A. Nelson. "Pulsed laser noise analysis and pump-probe signal detection with a data acquisition card." *Review of Scientific Instruments* 82, no. 12 (2011): 123108. © 2011 American Institute of Physics .

As Published: <http://dx.doi.org/10.1063/1.3669783>

Publisher: American Institute of Physics

Persistent URL: <http://hdl.handle.net/1721.1/82531>

Version: Final published version: final published article, as it appeared in a journal, conference proceedings, or other formally published context

Terms of Use: Article is made available in accordance with the publisher's policy and may be subject to US copyright law. Please refer to the publisher's site for terms of use.



Pulsed laser noise analysis and pump-probe signal detection with a data acquisition card

Christopher A. Werley, Stephanie M. Teo, and Keith A. Nelson


Citation: [Review of Scientific Instruments](#) **82**, 123108 (2011); doi: 10.1063/1.3669783

View online: <http://dx.doi.org/10.1063/1.3669783>

View Table of Contents: <http://scitation.aip.org/content/aip/journal/rsi/82/12?ver=pdfcov>

Published by the [AIP Publishing](#)

For all your variable temperature, solid state characterization needs....
... delivering state-of-the-art in technology and proven system solutions
for over 30 years!



The advertisement features the MMR Technologies logo on the left. Below it are four images of scientific instruments: a microscope, a Seebeck measurement system, a variable temperature microprobe system, and a Hall measurement system. Each image is accompanied by a red text label: 'Solutions for Optical Setups!', 'Seebeck Measurement Systems', 'Variable Temperature Microprobe Systems', and 'Hall Measurement Systems'.

Email: sales@mmr-tech.com Web: www.mmr-tech.com Phone: (650) 962-9622 Fax: (888) 522-1011

Pulsed laser noise analysis and pump-probe signal detection with a data acquisition card

Christopher A. Werley, Stephanie M. Teo, and Keith A. Nelson^{a)}

Department of Chemistry, Massachusetts Institute of Technology, Cambridge, Massachusetts 02139, USA

(Received 14 October 2011; accepted 26 November 2011; published online 16 December 2011)

A photodiode and data acquisition card whose sampling clock is synchronized to the repetition rate of a laser are used to measure the energy of each laser pulse. Simple analysis of the data yields the noise spectrum from very low frequencies up to half the repetition rate and quantifies the pulse energy distribution. When two photodiodes for balanced detection are used in combination with an optical modulator, the technique is capable of detecting very weak pump-probe signals ($\Delta I/I_0 \sim 10^{-5}$ at 1 kHz), with a sensitivity that is competitive with a lock-in amplifier. Detection with the data acquisition card is versatile and offers many advantages including full quantification of noise during each stage of signal processing, arbitrary digital filtering *in silico* after data collection is complete, direct readout of percent signal modulation, and easy adaptation for fast scanning of delay between pump and probe. © 2011 American Institute of Physics. [doi:10.1063/1.3669783]

I. INTRODUCTION

Pulsed lasers are ubiquitous in modern laboratories, and they make it possible to study ultrafast dynamics through pump-probe techniques. This technique has enabled an important and diverse set of experiments including short pulse characterization,¹ ultrafast motion of non-thermal electrons,² resolution of terahertz (THz) electric fields,³ and nuclear motion in proteins during electron transfer,⁴ among many others. The pulsed lasers used in these studies experience shot-to-shot and long-term fluctuations in pulse energy, which complicates the study of phenomena with small experimental signals. Here, we present a straightforward method that uses a data acquisition (DAQ) card to record the energy of every laser pulse for repetition rates less than ~ 500 kHz. Because the energy of every pulse is recorded, the method is very versatile and enables quantification of laser noise and arbitrary digital signal processing to measure weak pump-probe signals. Although DAQ card acquisition has been used by multiple laboratories in pump-probe experiments (e.g., see Refs. 5 and 6), we could find no paper detailing the implementation. We prefer this method to using a lock-in amplifier or boxcar integrator, and hope this demonstration will make it easier for others to adopt DAQ cards as a major tool for pump-probe signal acquisition.

In pump-probe measurements, the time-dependent response is recorded by stepping the delay between pump and probe pulses, and information is encoded as a pump-induced change in the probe pulse. The pump affects the real and/or imaginary parts of the sample's index of refraction, which, in turn, modifies the amplitude, phase, or polarization of the reflected or transmitted probe. When the phase or polarization is modified, interferometry or polarization sensitive detection is generally used to convert changes in phase or polarization to changes in probe intensity, which are sensed by the detector. Consequently, regardless of how the pump influences the

sample, the information is ultimately encoded in the energy of the probe pulse that reaches one or more detectors. When the pump is modulated, typically with every alternate pulse blocked, the probe light intensity I_0 reaching a detector with the pump blocked and the intensity I with the pump present can be measured and the fractional signal modulation $\Delta I/I_0$ can be retrieved by taking the ratio of consecutive probe pulse energies. It is very common that the desired signal is directly proportional to $\Delta I/I_0$ (e.g., see Refs. 7–10), and acquisition with the DAQ card gives rapid and straightforward access to this value.

II. EXPERIMENTAL METHODS

A photodiode detects the laser output, and the photodiode signal (a charge) is converted to a time-dependent voltage and amplified by a current preamplifier. The analog voltage output from the current preamplifier is digitized and recorded with the DAQ card [see Fig. 1(a)]. If the DAQ card is set to sample much faster than the repetition rate of the laser, the card behaves like a digital oscilloscope and records the time-evolution of the voltage. Figure 1(b) shows some example traces. In this demonstration, we used a titanium-sapphire laser with a regenerative amplifier to generate pulses at 1 kHz with a center wavelength of 800 nm, a pulse energy of 1.5 mJ, and a pulse duration of 80 fs. The photodiode was a low-noise, large area, unbiased silicon photodiode from Hamamatsu (model: S2281). We chose the current preamplifier (Stanford Research Systems, model: SR570) because of its low noise performance and filtering capabilities, whose use will be described below. The DAQ card, a National Instruments model: PCI-6281, had a maximum sampling rate of 625 kHz and an analog input with 18 bit resolution. At this bit depth, the discrete step size due to digitization, $76 \mu\text{V}$, is very small compared to laser noise [see Fig. 1(d)] and digitization effects can be ignored.

To record the energy of every laser pulse, it was important to measure some parameter that was directly proportional

^{a)} Author to whom correspondence should be addressed. Electronic mail: kanelson@mit.edu.

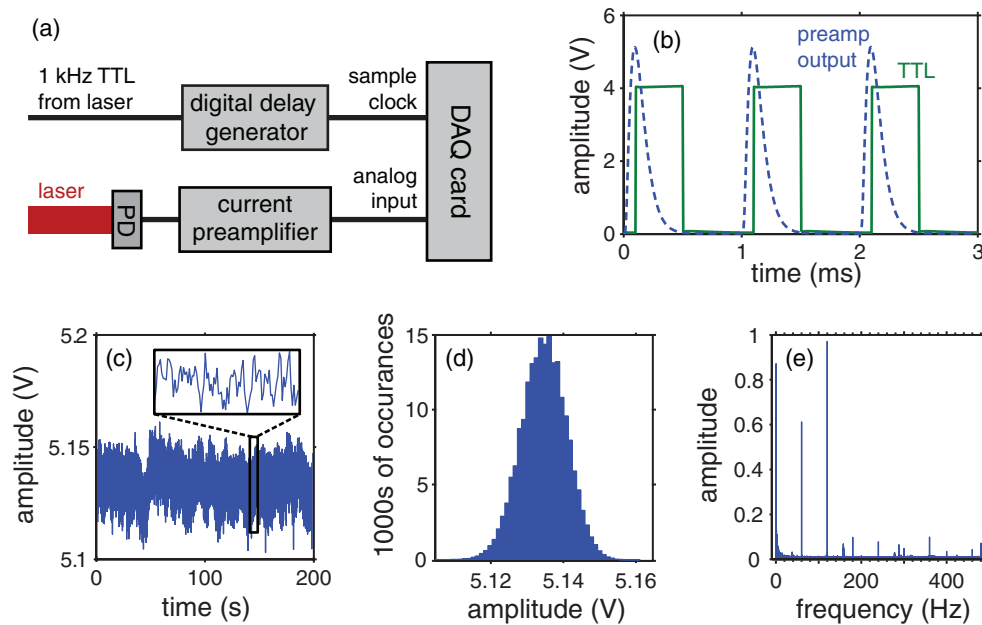


FIG. 1. (Color online) (a) The experimental setup for laser noise detection. The laser pulses are directed into a photodiode (PD) whose output is converted from current to voltage, amplified, and filtered to slow down the response. The measured voltage output from the current preamplifier is shown by the dashed line in (b). The sample clock of the DAQ card is given by an external TTL signal, which is synchronized to the laser. The TTL signal [shown as the solid line in (b)] is delayed such that the photodiode trace is sampled once at the peak of each pulse, effectively measuring the laser pulse energy. (c) The result of sampling 200,000 consecutive pulses, and the inset shows an expanded view of a short time period. (d) The distribution of the measured pulse energies. (e) The amplitude spectrum calculated by taking the Fourier transform of (c).

to the pulse energy. The peak voltage and integrated voltage of an electrical pulse both satisfy this criterion. We chose to measure peak voltage (which we confirmed was linearly proportional to pulse energy through all signal processing steps), as it was easier to acquire. The dashed traces in Fig. 1(b) show the input to the DAQ card, where a 3 kHz low-pass filter was applied by the preamplifier. The photodiode signal was filtered so that the voltage evolved on a slower timescale than the maximum sampling rate of the DAQ card, but still decayed to zero before the next laser pulse arrived at the photodiode. Alternative analog signal processing devices, such as a boxcar integrator or a sample and hold circuit, could be as effective as the current preamplifier with proper implementation. We considered these devices but chose the current preamplifier because it carefully handles the current signal from the photodiode and has excellent noise performance. It is also possible to implement this detection system without any of these analog devices. Pulse energy measurement works for a 1 kHz laser if the input impedance of the DAQ card is manually set to ~ 100 k Ω and the DAQ card's on-board amplifier is used prior to signal digitization. Although eliminating these analog devices reduces the expense of the system, it loses the versatility of filtering and amplification. These capabilities enable the detection of lower probe pulse energies and higher laser repetition rates, so including the current preamplifier, boxcar integrator, or other analog device is preferred.

One feature of the DAQ card is that an external timing signal can be used as the sampling clock. In this configuration, whenever the card detects the rising edge of a logic signal, it immediately (within 1.6 μ s, the delay is given approximately by the inverse of the sampling rate) records the voltage at the input of the analog-to-digital (A/D) converter. The transistor-

logic (TTL) signal used as the sample clock, shown as a solid line in Fig. 1(b), was synchronized to the repetition rate of the laser. The TTL pulse train was delayed relative to the laser output with a digital delay generator (Stanford Research Systems, model: DG535) such that the rising edge of the TTL pulse corresponded to the peak voltage of the preamplifier output [see Fig. 1(b)]. In this way, the phase between the detected pulses and the sampling clock was stable. The peak voltage was measured for every pulse, and this voltage was directly proportional to the laser pulse energy. The voltage corresponding to 200,000 consecutive laser pulses is shown in Fig. 1(c) and a histogram of the measured values is shown in Fig. 1(d). In this system, laser noise is much greater than noise from the electronics (measured as described in Sec. III), and essentially all the observed fluctuations in pulse energy come from the laser itself. In this data set, the laser was optimized for stability and displayed rms fluctuations of only 0.12%. This value, as well as pulse duration and pulse energy, is an important indicator of laser performance.

Figure 1(e) shows the noise spectrum of the laser calculated by taking the Fourier transform of the time trace in Fig. 1(c). The noise spectrum is very valuable because it reveals the frequencies of strong noise components, which should be avoided when modulating the pump for lock-in detection. Many features of the noise spectrum shown here are typical for the three Ti:Saph lasers we measured, including a constant background of white noise, the $1/f$ noise at low frequencies,¹¹ and the noise at the ac line frequency (60 Hz here) and its harmonics. The strong signal at 120 Hz, in particular, results from the rectifying power supply for the diodes in the pump laser for the regenerative amplifier. In addition, there were generally some noise components, like the peak at

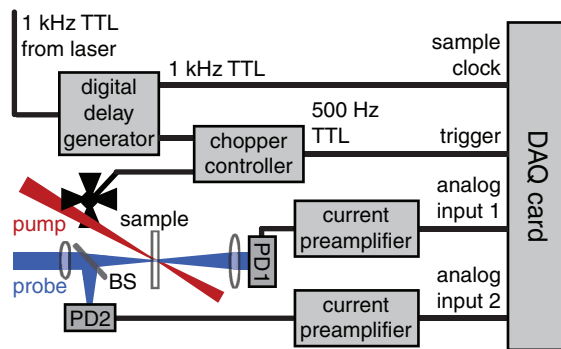


FIG. 2. (Color online) The experimental setup for taking pump-probe traces with the DAQ card. The pump, which can be variably delayed relative to the probe, is modulated at half the laser repetition rate with a chopper, which is synchronized to the laser. A beamsplitter (BS) placed before the sample splits off part of the probe beam to implement balanced detection. The current outputs of both photodiodes are converted to voltage, filtered, and amplified by the current preamplifiers prior to digitization by the DAQ card. The DAQ card sampling clock is synched to the laser so that every laser pulse energy is measured at each photodiode. The trigger signal from the chopper controller assures that the pump is always blocked when the first pulse energy is acquired.

~ 160 Hz and the cluster around 280 Hz, that were unique to the laser, day, or room.

To adapt the technique to measure pump-probe signals, a conceptually similar but more complicated setup is required (see Fig. 2). We employed standard strategies to achieve optimal noise reduction: balanced detection was implemented to suppress laser intensity fluctuations and the pump laser was modulated to shift the signal to higher frequencies and avoid $1/f$ noise. The digital delay generator, which was synchronized to the laser, provided the sample clock for the DAQ card and the synchronization frequency for the optical chopper. There were two photodiodes: one detected the probe before it interacted with the sample and the other detected after interaction. Each photodiode output was filtered and amplified as described above with a current preamplifier, and both the preamplifier outputs were recorded with the analog inputs of the DAQ card. We chopped the pump beam at 500 Hz, half the laser repetition rate, so that every other pump pulse was blocked. Because the digital delay generator set the sample clock, we measured the energy of every probe pulse arriving at each photodiode. Data acquisition by the DAQ card was triggered by the chopper controller, so that for every acquisition run, all the even numbered pulses had the pump present and odd numbered pulses had the pump blocked.

After all pulse energies are recorded, data processing in the computer is easily implemented. The signal from each photodiode for a pulse when the pump is present (pulse a) is normalized to the subsequent pulse when the pump is blocked (pulse b), correcting for differences in the optical paths. The normalized value from the diode after the sample (PD1) is divided by the normalized value from the diode preceding the sample (PD2), correcting for temporal fluctuations in the laser power. Finally, we subtract 1 to retrieve the modulation:

$$\frac{\Delta I}{I_0} = \frac{PD1_a}{PD1_b} \bigg/ \frac{PD2_a}{PD2_b} - 1. \quad (1)$$

It is convenient that the output of this processing is $\Delta I/I_0$, the physically relevant quantity in many experiments. Different detection schemes, such as balancing with a Wollaston prism or dark background detection, require different mathematical processing that can easily be implemented in software.

The maximum repetition rate laser to which this method can be applied depends on the photodiode, current preamplifier, and DAQ card used. For the hardware described above, the rate is limited by the DAQ card, which has a single analog-to-digital converter. The limit is set by the time it takes to sample analog input 1 followed by analog input 2, $\sim 7 \mu\text{s}$ in practice. Because performance is best when the signal detected by each analog input channel is similar, the voltage trace should evolve on a significantly slower timescale than the sampling rate, and we found 20 kHz to be a practical upper limit. With a biased PIN (P-doped: intrinsically doped: N-doped) photodiode, enough probe input power, and a simultaneous-sampling DAQ card with a sufficiently high sampling rate, it should be possible to push this method up to 500 kHz repetition rate lasers or beyond.

III. RESULTS AND DISCUSSION

A. Signal processing and noise

An advantage of the DAQ card detection system is that the noise can be quantified after each noise-suppression technique (i.e., chopping, balancing, and averaging) is implemented. Figure 3 shows the noise spectrum and histogram of values for different schemes, where each value has been normalized to the mean. To generate these plots, 200,000 pulses of 400 nm light were collected from a pair of photodiodes, as shown in Fig. 2, and the values were processed in different ways. The number in the upper right of each histogram is the standard deviation of the distribution, which gives the rms noise. The boxed number in the lower right of each spectrum is the factor by which the spectral amplitude was multiplied in that subplot. Figures 3(a) and 3(b) show the spectrum and histogram for the unprocessed laser output measured at a single photodiode. When these data were measured, the laser was much noisier than for the data shown in Fig. 1, and the distribution of values extends well beyond the bounds on the axes. Figures 3(c) and 3(d) show the output when every laser pulse from a single photodiode is divided by the subsequent pulse, simulating chopping. The frequency spectrum only extends to 250 Hz because pairs of pulses are combined to make a single value. Chopping can be thought of as a high-pass filter: it suppresses low-frequency noise but high-frequency noise is only slightly reduced. Figures 3(e) and 3(f) show the output if pulse energies are recorded by a pair of photodiodes, and one photodiode output is normalized by the other. This greatly suppresses noise at all frequencies, as can be easily seen by the much narrower distribution of values and the greater than 10-fold reduction in noise from the unprocessed data. Figures 3(g) and 3(h) show the result of the operations in Eq. (1), which incorporates balancing and chopping. This displays good overall noise suppression and excellent suppression at low frequencies, which is why these

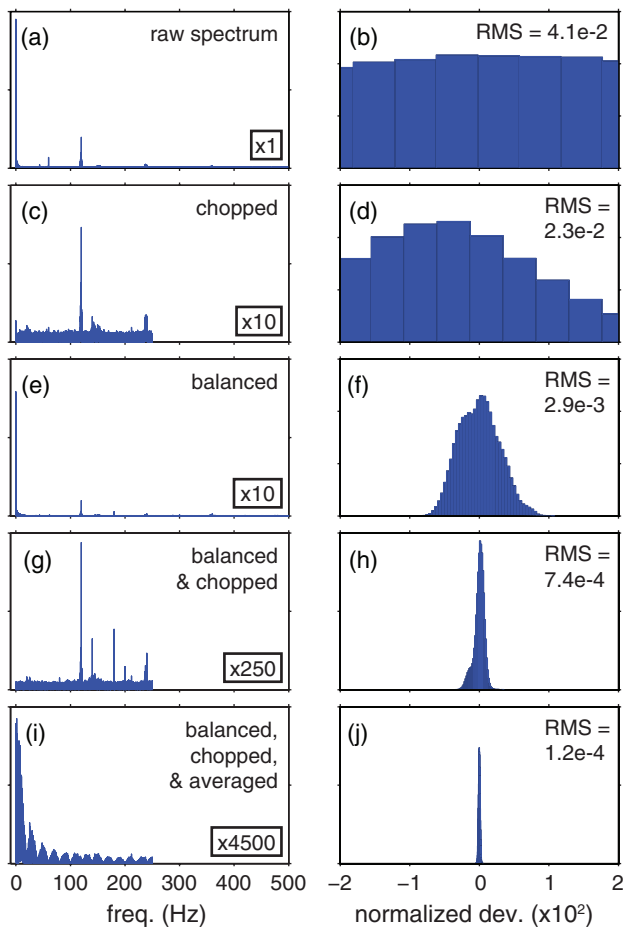


FIG. 3. (Color online) The noise amplitude spectrum and histogram of measured values normalized to the mean for 200,000 pulses of 400 nm light processed in different ways. The amplitude for each spectrum was multiplied by the boxed factor in the lower right of the plot. The rms fluctuation value in the upper right of the histogram plots is the standard deviation of the distribution, which reflects the efficacy of each processing step. (a) and (b) are from the raw pulse energies with no processing. For (c) and (d), each pulse from one photodiode was divided by the subsequent pulse to mimic chopping. In (e) and (f), the outputs from two photodiodes, as shown in Fig. 2, were divided to mimic balancing. (g) and (h) show the results of dividing one photodiode output by the other and then dividing ratios from successive time points to mimic chopping and balancing. (i) and (j) have the same processing as in (g) and (h), but the entire trace is convolved with a rectangle function 25 values long to mimic averaging.

noise suppression techniques are so widely implemented. It is possible to further reduce the noise by digital filtering of the data. Figures 3(i) and 3(j) show the result of the simplest digital filter: unweighted averaging. This can be thought of as convolving the pulse time sequence with a rectangular function, which is equivalent to multiplying by a sinc function in the frequency domain, as can be clearly seen in Fig. 3(i). We chose the number of pulses to average such that an integer number of cycles of the largest noise components were averaged over, almost completely suppressing those noise components. In other words, we chose the width of the convolving rectangular function so that the nodes of the sinc function in the frequency domain fell on top of the largest noise components. Here, we averaged 25 pulse pairs, with a total averaging time of 50 ms or three cycles of the line frequency, which suppressed noise at 60 Hz and its harmonics. The 5.5-fold noise

suppression between Figs. 3(h) and 3(j) is roughly consistent with \sqrt{n} scaling predicted for averaging. Figure 3(j) has an rms noise of only 1.2×10^{-4} , which highlights the capability to detect weak signals even with short averaging times when using this measurement system.

Even though the laser noise is significantly reduced by balancing and chopping, laser fluctuations are still the dominant noise source. Shot noise resulting from Poisson's statistics in the probe has a magnitude of $1/\sqrt{N}$, where N is the number of photons in the laser pulse.¹² If we use pulse energies at the high end of the linear response regime of our photodiode, roughly 0.5 nJ/pulse at 400 nm or $\sim 10^9$ photons/pulse, shot noise is around 3×10^{-5} for a single pulse. Because the shot noise for each pulse measured is uncorrelated, the noise variances add when performing the mathematical operations in Eq. (1), leading to a total contribution from shot noise of 6×10^{-5} , which is more than an order of magnitude smaller than fluctuations not fully suppressed by balancing and chopping. To quantify the noise arising from the measurement electronics, we blocked all light from hitting the photodiodes and used a setting on the current preamplifiers that generates a small dc offset current. This current was amplified and detected at 1 kHz by the DAQ card in the same way as the real data, then processed as if balancing and chopping were implemented. With well shielded cabling and good connections between the photodiode and the preamplifier, the normalized rms deviation was 9×10^{-5} , significantly smaller than the laser noise from the balanced and chopped signal. When a very low-noise laser is used, such as that shown in Fig. 1 where the normalized rms deviation is only 0.13%, it is possible for the balanced and chopped output to have an rms deviation of $\sim 3 \times 10^{-4}$ (data not shown), still significantly larger than noise from the electronics or shot noise. Thus, the performance of the detection electronics is sufficiently good that measurements are limited by pointing and shot-to-shot energy fluctuations in the laser.

B. Comparison with a lock-in amplifier

Lock-in amplifiers¹³ are often used to measure pump-probe signals. Figure 4 shows a direct comparison of terahertz electric field time traces measured using a lock-in amplifier and the DAQ card system. In these measurements, the terahertz field induced birefringence in an electro-optic crystal, changing the polarization of a transmitted optical pulse whose orthogonal polarization components were directed to two photodiodes for balanced detection.¹⁴ For both the measurements, we used the 1 kHz Ti:Saph laser system described above and implemented balanced detection and chopping at 500 Hz. For the lock-in amplifier, balancing was implemented by sending both signals into the instrument, a Stanford Research Systems SR810, which subtracted the inputs before performing additional signal processing. In this scheme, careful balancing is required for optimal noise suppression. Slow drift of laser pointing unbalances the diodes, which can adversely affect performance. For the DAQ card system, the mathematical divisions in Eq. (1) make careful balancing unnecessary and significantly reduce the sensitivity to drift in the balancing ratio.

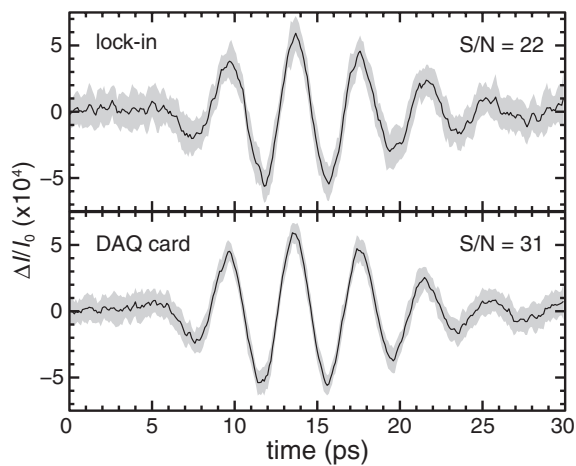


FIG. 4. The time trace of a multi-cycle THz pulse with a center-frequency of 250 GHz measured using a lock-in amplifier (top panel) and the DAQ card measurement system (bottom panel). The total measurement time was the same for both methods. For each method, the trace was measured 25 times. The black is the average and the gray is $\pm\sigma$ for each time delay, so that 68% of measurements fall within the gray region. The S/N for each method compares the average uncertainty (which was roughly independent of time delay) to the peak signal.

In a lock-in amplifier, typically both the time constant τ and the filter roll-off are programmable. The roll-off reflects the number n of sequential RC-type filters the lock-in signal passes through ($n = 1$ for 6 dB/octave, $n = 2$ for 12 dB/octave, $n = 3$ for 18 dB/octave, etc.). Passing through n filters can be described mathematically as convolving the lock-in signal with an exponential function n times, or convolving the signal with the function

$$f(t) = \frac{t^{n-1}}{(n-1)!} e^{-t/\tau} u(t), \quad (2)$$

with $u(t)$ the Heaviside step function.¹⁵ The lock-in output at a time t most strongly reflects the peak of this function, which occurred earlier at a time $t - (n-1)\tau$. It takes more time constants for the majority of the signal to decay out of the buffer when changing conditions (e.g., the time delay in a pump-probe measurement). In our measurement, we chose $\tau = 30$ ms and a fourth order, 24 dB/octave filter. We waited 8 time constants, 240 ms, so that there was a roughly 4% contribution to the signal at each time delay from the previous time step. A total of 250 pulses were averaged for the DAQ card, which never has parasitic contributions from previous time delays. Using these settings, the number of pulses averaged at each delay and the total scan time were roughly the same for both the methods. The time trace was collected 25 times for each method to build up statistics for signal-to-noise ratio (S/N) comparisons. In Fig. 4, the black line shows the average of the traces and the gray area shows one standard deviation (σ) on either side of the average for each time delay, giving the spread in the measurements. As can be seen from the figure, the traces look very similar and the data have a similar spread. The standard deviation was basically independent of time delay for both the methods, so the S/N was calculated with the maximum signal and the standard deviation averaged over the delay time as: $S/N = \max(\Delta I/I_0) / (\sqrt{n} \sigma)$. The S/N is about 40% better for the DAQ card here; however,

in our experience the relative performance of the two techniques depends on the nature of the laser fluctuations, and overall both methods have similar minimum-signal detection thresholds.

C. Rapid scanning

In spite of the similarity in detection thresholds for long averaging times, the DAQ card system has some advantages at short averaging times. Because the lock-in amplifier multiplies the input voltage by a sine wave and convolves with the expression in Eq. (2), it is necessary for the lock-in time constant to be significantly longer than the modulation period. If this is not the case and the expression in Eq. (2) evolves significantly during a single modulation period, quantification of the signal amplitude will be impaired. This is not the case in the DAQ card system because it uses equally weighted, rectangular function averaging. The minimum averaging time is one modulation period, or two laser pulses if modulation occurs at half the repetition rate. Another disadvantage of the exponential averaging implemented by the lock-in is that when stepping to a new time delay in a pump-probe measurement, it is necessary to wait many time constants for the signal from the previous time delay to decay away. This is why we had the 8τ waiting time when we took the lock-in trace in Fig. 4. No waiting is necessary with rectangular function averaging, so a time trace can be acquired more quickly with the DAQ card.

A capability made possible by the short averaging time required by the DAQ card system is rapid scanning. To implement this, we used an ILS150PP delay stage and ESP300 stage controller from Newport. The stage was accelerated to a target velocity, at which point the DAQ card acquired signal continuously until the desired time delay was reached. Data acquisition was then stopped, the stage was quickly returned to the starting position, and the whole process was performed repeatedly. Knowing the stage velocity and laser repetition rate, it is straightforward to measure femtosecond or picosecond time traces with accurate time dynamics, assuming the signal is large enough to measure with minimal averaging. We were able to display 10 ps time scans and their corresponding frequency spectra at a refresh rate of ~ 1 Hz (data not shown). This rapid scanning and real-time feedback was very useful for improving optical alignment and optimizing pump-probe overlap, pulse compression, and pump pulse spatiotemporal shaping. The delay stage and controller we used to implement fast scanning were not chosen with this application in mind, and a delay stage with a faster acceleration will enable even shorter acquisition times.

D. Differential chopping

When chopping low repetition rate lasers (i.e., ~ 10 kHz or below), generally one requires that the chopping is implemented such that pump pulses either pass completely through the chopper wheel without clipping or are fully blocked. This ensures that the pump intensity profile at the sample is never altered. To implement this cleanly, the pump is chopped at an even integer fraction of the repetition rate R (e.g., $R/2$:

one passed, one blocked; $R/4$: two passed, two blocked; $R/6$; etc.). When two pump lasers are directed into the sample, the coupling between their induced effects can be sensitively detected by implementing differential chopping. In this scheme, the pumps are chopped at different frequencies, and the signal is detected with a lock-in amplifier at the difference frequency. If one requires chopping at even integer fractions, the fastest difference frequency that is not degenerate with one of the fundamental modulation frequencies is achieved by chopping one pump at $R/4$, the other at $R/6$, and detecting at $R/12$, which extracts only the signal resulting from the coupling between the pumps. The noise can be a problem because of the low detection frequency, and it takes additional work to extract signals from just one pump or the other. Although we have not tested it, we believe that the DAQ card method offers an elegant alternative. In the DAQ card scheme, one pump would be chopped at $R/2$ and the other at $R/4$. Looking at four sequential probe pulses, the state would be S_{++} , S_{+-} , S_{-+} , and S_{--} , where “+” means the pump is present and “-” means the pump is absent. From these four values, all the relevant information can be extracted. The signal resulting from both the pumps, the first pump only, the second pump only, and the coupling between the pumps is given by $S_{++}/S_{--} - 1$, $S_{+-}/S_{--} - 1$, $S_{-+}/S_{--} - 1$, and $(S_{++} - S_{+-} - S_{-+} + S_{--})/S_{--}$, respectively. In addition, all four signals are detected at $R/4$, a relatively high frequency, leading to effective noise suppression. As a result, the DAQ card system offers multiple advantages in a differential chopping scheme.

IV. CONCLUSIONS

The detection system described here, which consists of a photodiode, a current preamplifier, and a data acquisition card clocked by the laser, is a versatile and useful tool for pump-probe experiments. When the DAQ sampling rate is driven by its internal clock, the system acts like an oscilloscope. When the DAQ card's sampling clock is a TTL pulse train synchronized to the laser repetition rate, the intensity of every pulse is measured. This enables laser noise quantification and measurement of the noise spectrum, much like a spectrum analyzer. When the DAQ card system is used with pump modulation and balanced detection, it is able to measure very small signals in much the same way as a lock-in amplifier. Because the energy of every laser pulse is measured, it is possible to perform arbitrary linear or nonlinear filtering on the data to further reduce the noise. For example, with a more unstable laser it might be beneficial to set a threshold so that abnormally large or small pulses would be discarded and not included when calculating average behavior, as has been done

previously (e.g., see Ref 5). A final advantage is fast scanning, which facilitates the optimization of optical alignment and real-time feedback on the fast dynamics in the system.

In addition to these diverse capabilities, data processing in the DAQ system is intuitive. Signal and reference are measured both through the sample and avoiding the sample, and everything is divided to cancel out temporal fluctuations and path differences. This processing scheme, which is implemented in many common instruments, is simple to understand for experimenters new to this kind of technique. In addition, the direct output is $\Delta I/I_0$, which is useful for comparing signal magnitude across different experiments and is often proportional to some relevant physical quantity of the system. Combined with the quantification of laser noise, this helps build intuition about the system under study and the experimental apparatus. DAQ cards have been and are used for pump-probe measurements by various laboratories, but they are not as ubiquitous as lock-in amplifiers. Because of its conceptual simplicity and general versatility, we believe that the DAQ card measurement system merits wider adoption in the pump-probe community.

ACKNOWLEDGMENTS

The authors would like to thank Vasily Temnov for valuable discussions. The work described here was supported by ONR Grant No. N00014-09-1-1103 and a National Science Foundation Graduate Research Fellowship (C.A.W.).

¹E. P. Ippen and C. V. Shank, *Appl. Phys. Lett.* **27**, 488 (1975).

²S. D. Brorson, J. G. Fujimoto, and E. P. Ippen, *Phys. Rev. Lett.* **59**, 1962 (1987).

³D. H. Auston and M. C. Nuss, *IEEE J. Quantum Electron.* **24**, 184 (1988).

⁴M. H. Vos, F. Rappaport, J.-C. Lambry, J. Breton, and J.-L. Martin, *Nature (London)* **363**, 320 (1993).

⁵S. Ruhman, A. G. Joly, and K. A. Nelson, *IEEE J. Quantum Electron.* **24**, 460 (1988).

⁶M. Lim, T. A. Jackson, and P. A. Anfinrud, *Proc. Natl. Acad. Sci. USA* **90**, 5801 (1993).

⁷N. C. J. van der Valk, T. Wenckebach, and P. C. M. Planken, *J. Opt. Soc. Am. B* **21**, 622 (2004).

⁸O. B. Wright, B. Perrin, O. Matsuda, and V. E. Gusev, *Phys. Rev. B* **78**, 024303 (2008).

⁹H. E. Lessing and A. von Jena, *Chem. Phys. Lett.* **42**, 213 (1976).

¹⁰G. D. Goodno, G. Dadusc, and R. J. D. Miller, *J. Opt. Soc. Am. B* **15**, 1791 (1998).

¹¹P. Bak, C. Tang, and K. Wiesenfeld, *Phys. Rev. Lett.* **59**, 381 (1987).

¹²A. Yariv, *Introduction to Optical Electronics* (Holt, Rinehart and Winston, New York, 1971).

¹³P. A. Temple, *Am. J. Phys.* **43**, 801 (1975).

¹⁴J. A. Valdmanis, G. A. Mourou, and C. W. Gabel, *IEEE J. Quantum Electron.* **QE-19**, 664 (1983).

¹⁵A. V. Oppenheim, A. S. Willsky, and S. H. Nawab, *Signals and Systems*, 2nd ed. (Prentice Hall, Upper Saddle River, 1997)